Supporting Information

Chitosan-Templated Pt Nanocatalyst Loaded Mesoporous SnO_2 Nanofibers: Superior Chemiresistor toward Acetone Molecules

Yong Jin Jeong, Won-Tae Koo, Ji-Soo Jang, Dong-Ha Kim, Hee-Jin Cho, and Il-Doo Kim*

Department of Materials Science and Engineering, Korea Advanced Institute of Science and Technology (KAIST), 291 Daehak-ro, Yuseong-gu, Daejeon 34141, Korea

*Corresponding author e-mail: idkim@kaist.ac.kr

Table of Contents

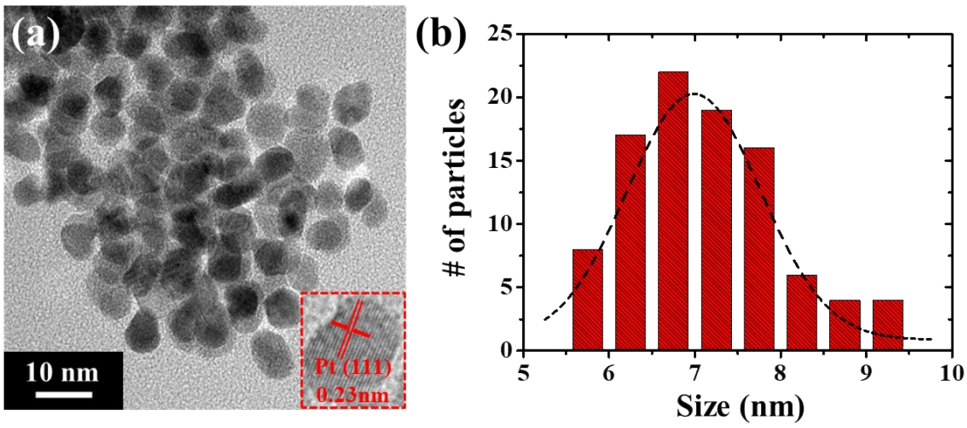

Figure. S1 a) HRTEM image and b) size distribution of polyol-Pt NPs.

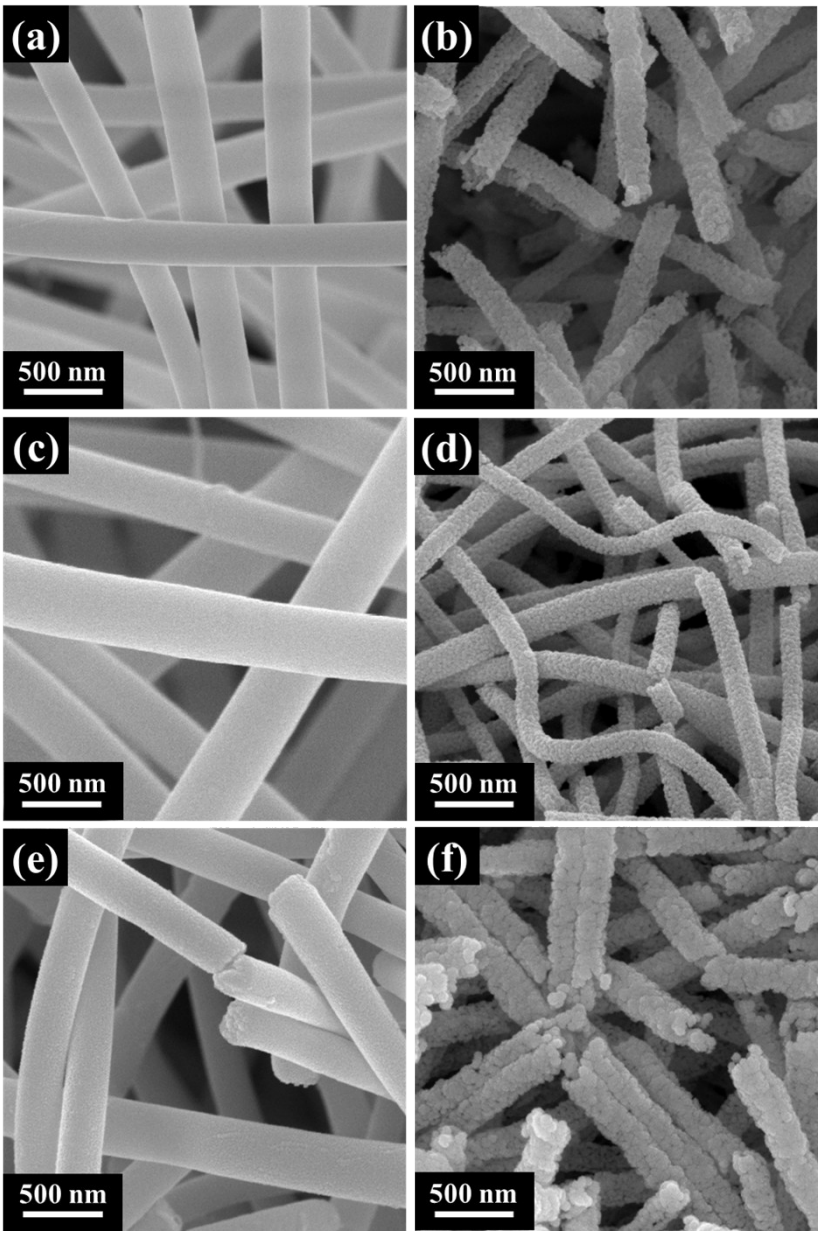

Figure. S2 SEM images: a) as-spun Sn precursor/PVP NFs, b) dense SnO_2 NFs, c) as-spun Sn precursor/PVP/CS NFs, d) CS@SnO_2 NFs, e) as-spun Sn precursor/PVP/polyol-Pt, and f) polyol-Pt@SnO_2 NFs.

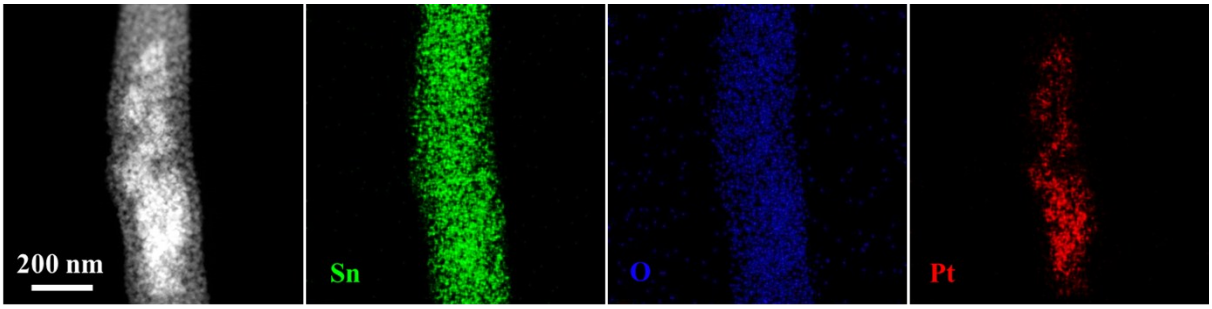

Figure. S3 EDS elemental mapping images for Sn, O, and Pt in polyol-Pt@SnO_2 NFs.

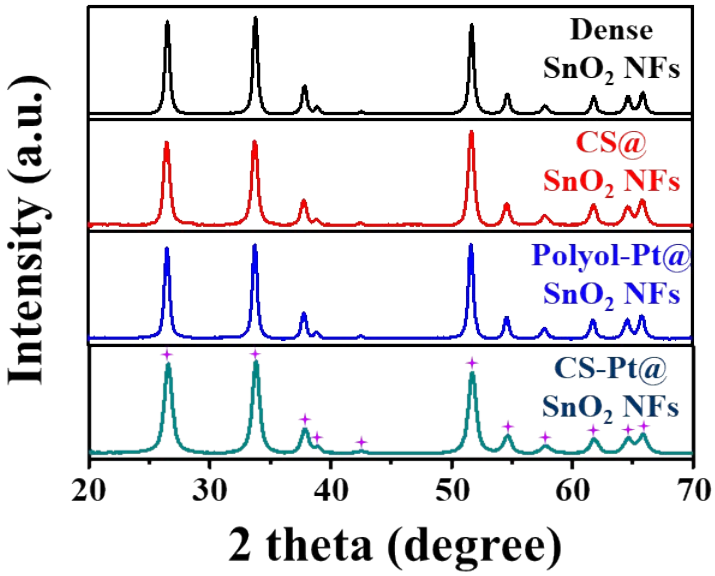

Figure. S4 XRD analysis of dense SnO_2 NFs, CS@SnO_2 NFs, polyol-Pt@SnO_2 NFs, and CS-Pt@SnO_2 NFs.

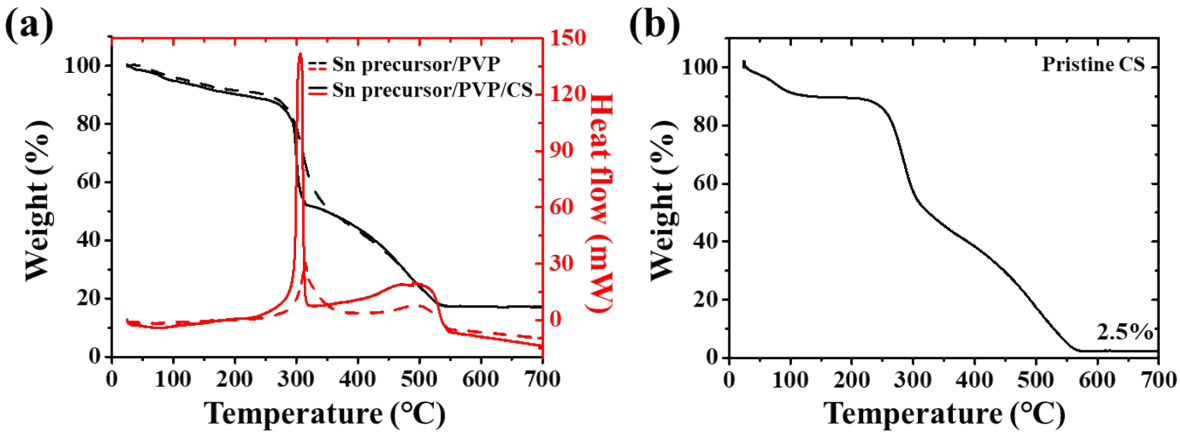

Figure. S5 Thermal gravimetric and differential scanning calorimetry analysis: a) as-spun Sn precursor/PVP and Sn precursor/PVP/CS NFs, and b) pristine CS.

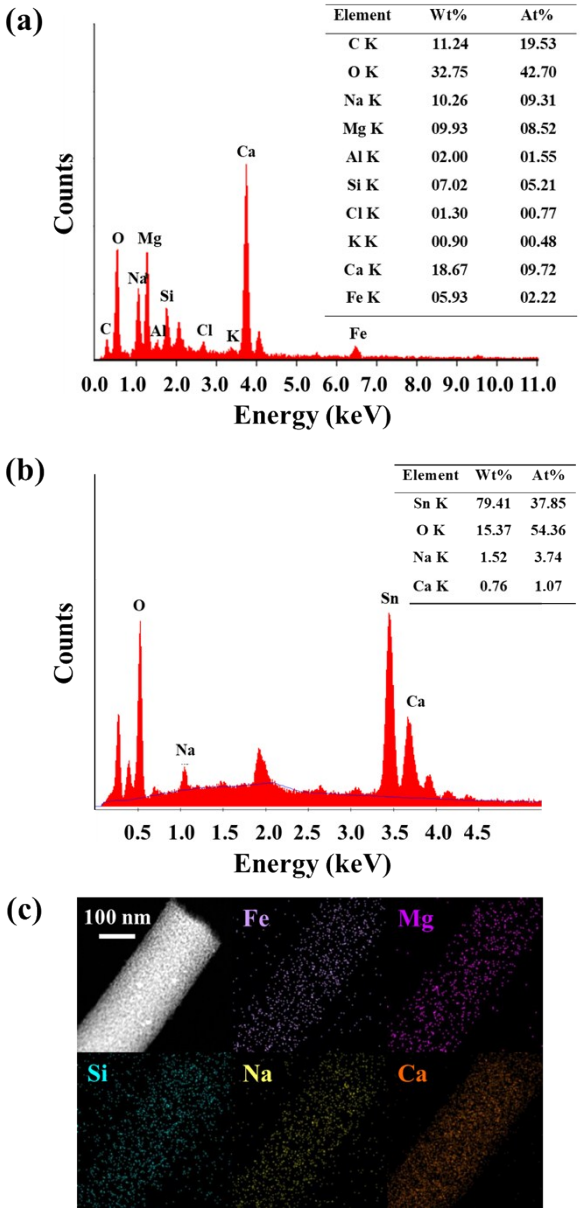

Figure. S6 EDS analysis of a) CS residues and b) CS-Pt@SnO_2 NFs. c) EDS elemental mapping images for Fe, Mg, Si, Na, and Ca contained in CS-Pt@SnO_2 NFs.

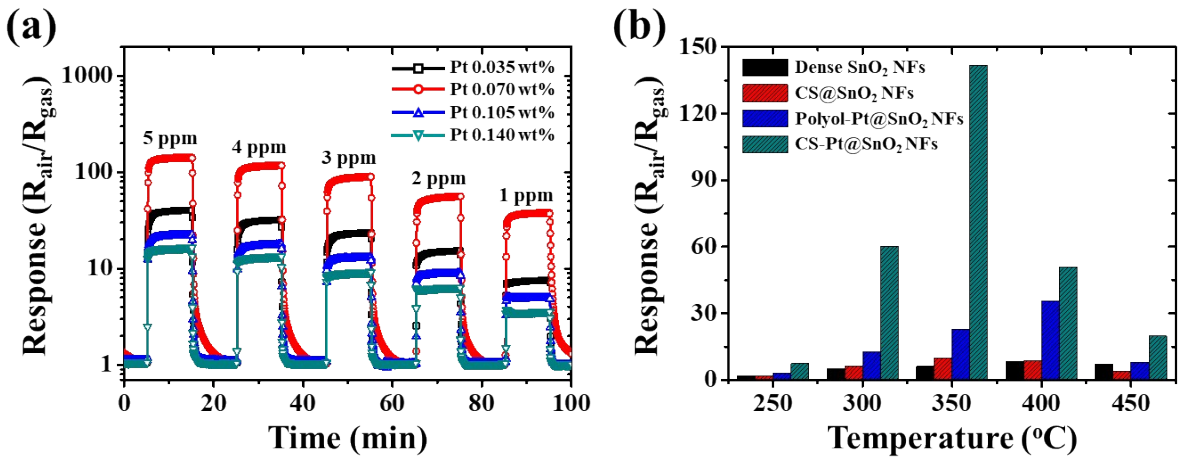

Figure. S7 a) Dynamic acetone sensing performance of CS-Pt@SnO_2 NFs for Pt amounts in the range of 0.035–0.140 wt% at 350 °C, and b) response of CS-Pt@SnO_2 NFs, polyol-Pt@SnO_2 NFs, CS@SnO_2 NFs, and dense SnO_2 NFs toward 5 ppm of acetone at different temperatures (250–450 °C).

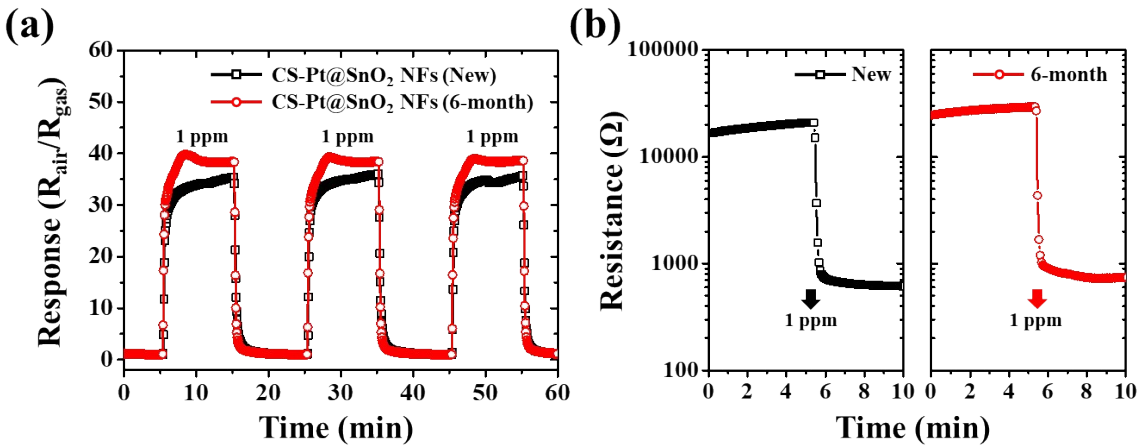

Figure. S8 a) Response and b) resistance variation of CS-Pt@SnO_2 NFs toward 1 ppm of acetone at 350 ℃ and 90% RH using the new and the 6-month old sensors.

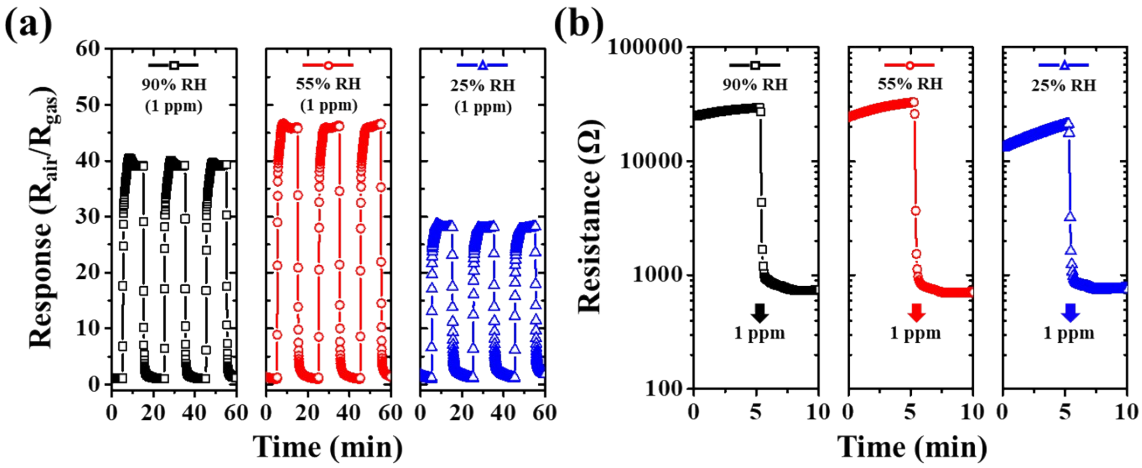

Figure. S9 a) Response and b) resistance variation of CS-Pt@SnO_2 NFs toward 1 ppm of acetone at 90, 55, and 25% RH.

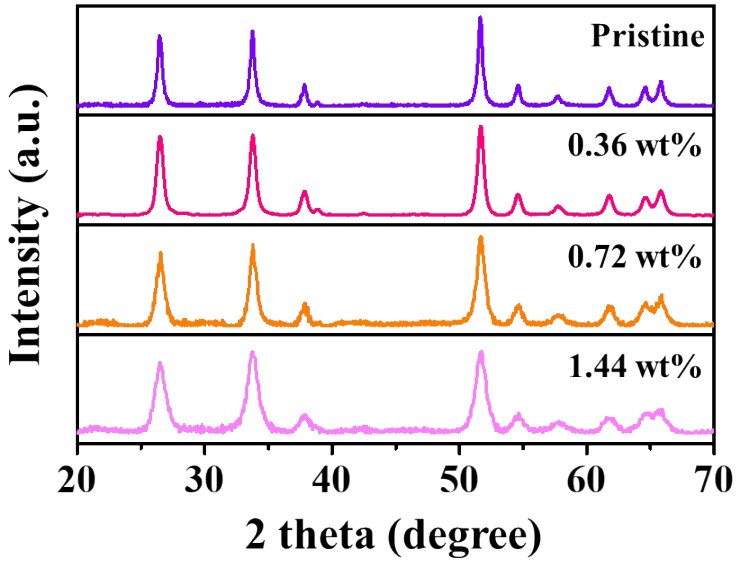

Figure. S10 XRD analysis of CS@SnO_2 NFs containing 0–1.44 wt% of CS.

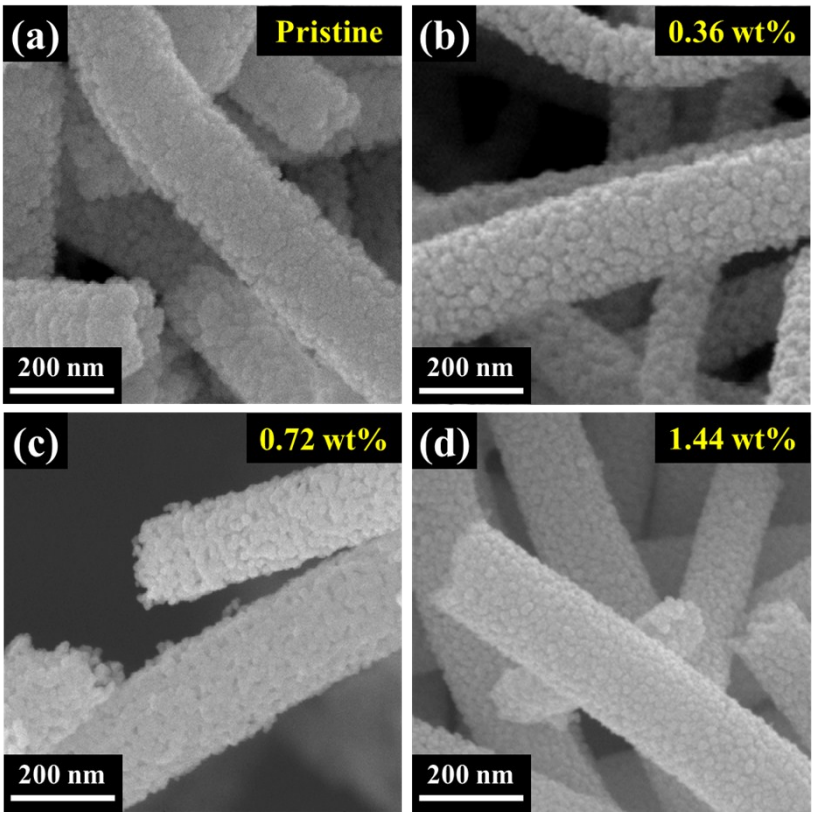

Figure. S11 SEM images of a) pristine SnO_2 NFs, b) 0.36 wt% CS loaded SnO_2 NFs, c) 0.72 wt% CS loaded SnO_2 NFs, and d) 1.44 wt% CS loaded SnO_2 NFs.

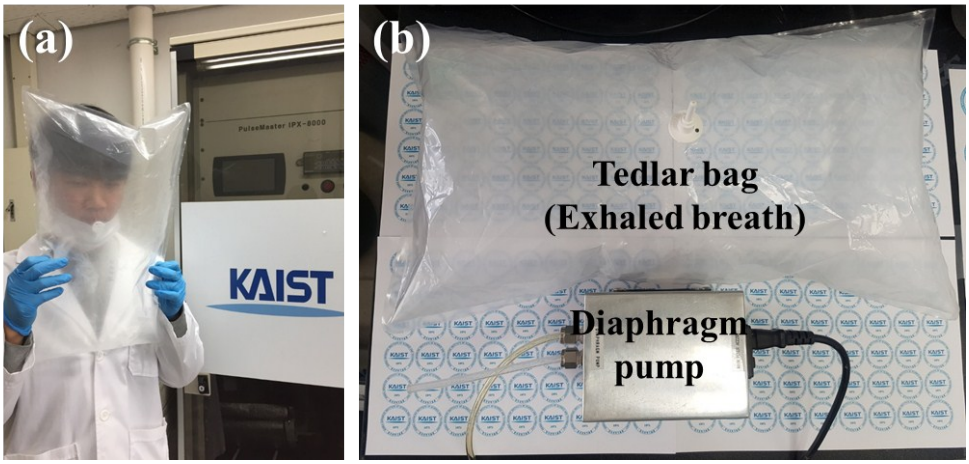

Figure. S12 a) Exhaled breath sampling in a tedlar bag, and b) exhaled breath sample and a diaphragm pump.

Table. S1 Recently reported gas sensors for detecting acetone in highly humid ambient.

Gas species	Materials	Optimal temperature	Relative humidity	Response	Response definition	Ref.
Acetone	La-Fe_2O_3 NTs	240 °C	95% RH	6 at 50 ppm	R_{air}/R_{gas}	1
	Au modified In_2O_3	340 °C	80% RH	42.4 at 5 ppm	R_{air}/R_{gas}	2
	Si-doped WO_3	400 °C	90% RH	1.5 at 0.6 ppm	$R_{air}/R_{gas} - 1$	3
	Pt-AF_WO_3 NFs	350 °C	90% RH	153 at 5 ppm	R_{air}/R_{gas}	4
	Rh_2O_3–WO_3 NFs	350 °C	95% RH	11.2 at 1 ppm	R_{air}/R_{gas}	5
	PtO_2-SnO_2 MCNFs	400 °C	95% RH	194.15 at 5 ppm	R_{air}/R_{gas}	6
	Pt-PS_SnO_2 NTs	350 °C	90% RH	34.8 at 1 ppm	R_{air}/R_{gas}	7
	PtRh-WO_3 NFs	350 °C	90% RH	104 at 1 ppm	R_{air}/R_{gas}	8
	CS-Pt@SnO_2 NFs	350 °C	90% RH	141.92 at 5 ppm	R_{air}/R_{gas}	this work

References

1 H. Shan, C. Liu, L. Liu, S. Li, L. Wang, X. Zhang, X. Bo and X. Chi, *Sens. Actuators, B*, 2013, **184**, 243-247.

2 R. Xing, Q. Li, L. Xia, J. Song, L. Xu, J. Zhang, Y. Xie and H. Song, *Nanoscale*, 2015, **7**, 13051-13060.

3 M. Righettoni, A. Tricoli and S. E. Pratsinis, *Anal. Chem.*, 2010, **82**, 3581-3587.

4 S. J. Kim, S. J. Choi, J. S. Jang, N. H. Kim, M. Hakim, H. L. Tuller and I. D. Kim, *ACS nano*, 2016, **10**, 5891-5899.

5 N. H. Kim, S. J. Choi, S. J. Kim, H. J. Cho, J. S. Jang, W. T. Koo, M. Kim and I. D. Kim, *Sens. Actuators, B*, 2016, **224**, 185-192.

6 Y. J. Jeong, W. T. Koo, J. S. Jang, D. H. Kim, M. H. Kim and I. D. Kim, *ACS Appl. Mater. Interfaces*, 2018, **10**, 2016–2025

7 J. S. Jang, S. J. Choi, S. J. Kim, M. Hakim and I. D. Kim, *Adv. Funct. Mater.*, 2016, **26**, 4740-4748.

8 S. J. Kim, S. J. Choi, J. S. Jang, H. J. Cho, W. T. Koo, H. L. Tuller and I. D. Kim, *Adv. Mater.*, 2017, **29**, 1700737